Convective Cold Pools over the Atlas Mountains and their Influence on the Saharan Heat Low

Robert Redl[1] (robert.redl@lmu.de), Peter Knippertz[2], Andreas H. Fink[2]

[1])Meteorological Institute, LMU Munich, Munich, Germany; [2])Institute of Meteorology and Climate Research, Karlsruhe Institute of Technology (KIT), Karlsruhe, Germany

Motivation and Objectives

With the current state of research, three pathways of ventilation for the summertime Saharan Heat Low (SHL) are known (Figure 1):

- In the south, the African Easterly Waves (AEWs) with their monsoon surges and convective cold pools from Mesoscale Convective Systems (MCSs).
- In the north, cold surges from the Mediterranean Sea related to upper-level troughs and lee cyclogenesis.
- In the west, the Atlantic inflow modulates the SHL.

Research Question: Are convectively driven cold pools from the Atlas Mountains an additional pathway of ventilation?

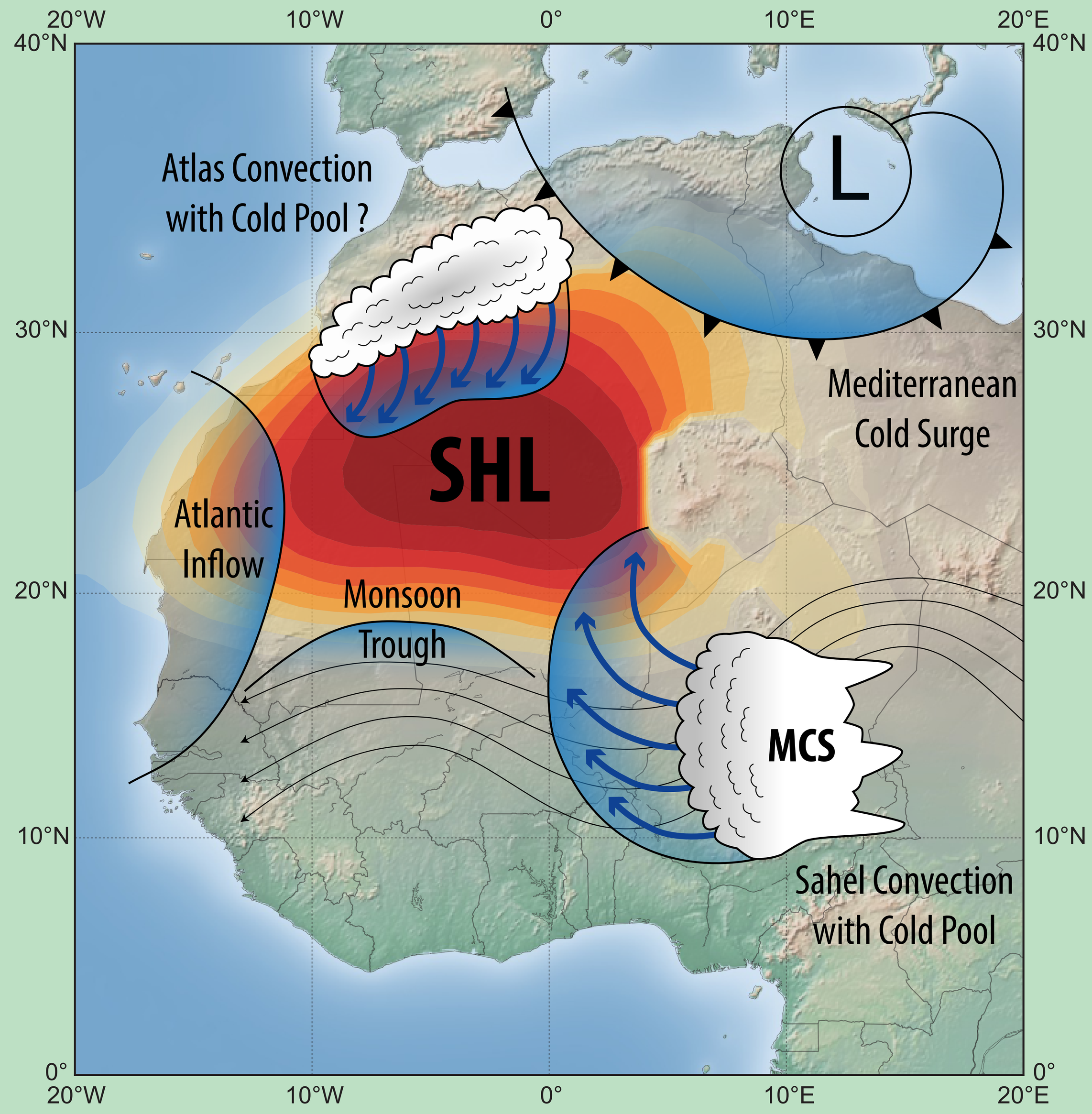

Figure 1: Processes relevant for the variability of the SHL on the sub-monthly time scale. Included are the position of the SHL in August, streamlines of the AEJ with an MCS in a realistic position relative to the AEW, the monsoon trough, the Atlantic inflow, cold surges from the Mediterranean, and convection over the Atlas Mountains, which is proposed to be relevant as well.

Domain and Data

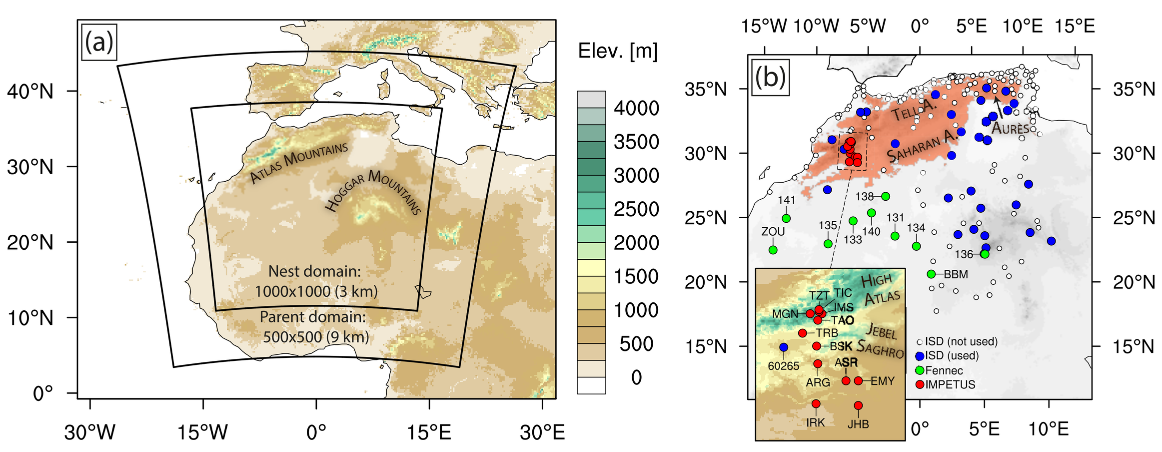

Figure 2: Model domain, location of ground observations, and important geographical names. (a) Model parent and nest domains with orography. (b) Nest domain including the locations of ground observations from the datasets ISD, Fennec, and IMPETUS. The red shading indicates grid points over the Atlas Mountains with an elevation of more than 500 m.

In addition to the ground observations from stations shown in Fig. 2b, more than 100,000 satellite overpasses from AMSU-B and MHS instruments were used.

Summary

- **From May to September, about 6 large cold pool events per month are detected over the Atlas Mountains.**
- **These events are often clustered into periods of several days length.**
- **Cold pools increase surface pressure and transport moisture into the Sahara over multiple days.**
- **Cold pools contribute to the variability of the heat low on the synoptic time scale.**

Download References:

Redl, R., A. H. Fink, and P. Knippertz (2015), An Objective Detection Method for Convective Cold Pool Events and Its Application to Northern Africa, Mon. Weather Rev., 143(12), 5055–5072, doi:10.1175/MWR-D-15-0223.1.

Redl, R., P. Knippertz, and A. H. Fink (2016), Weakening and Moistening of the Summertime Saharan Heat Low through Convective Cold Pools from the Atlas Mountains, J. Geophys. Res. Atmos., doi:10.1002/2015JD024443.

Part 1: Frequency of Large-Scale Convective Cold Pool Events

Novel Objective Cold Pool Detection Algorithm

Firstly, the regularity of cold pool events in Northwest Africa is addressed by the creation of a multi-year climatology.

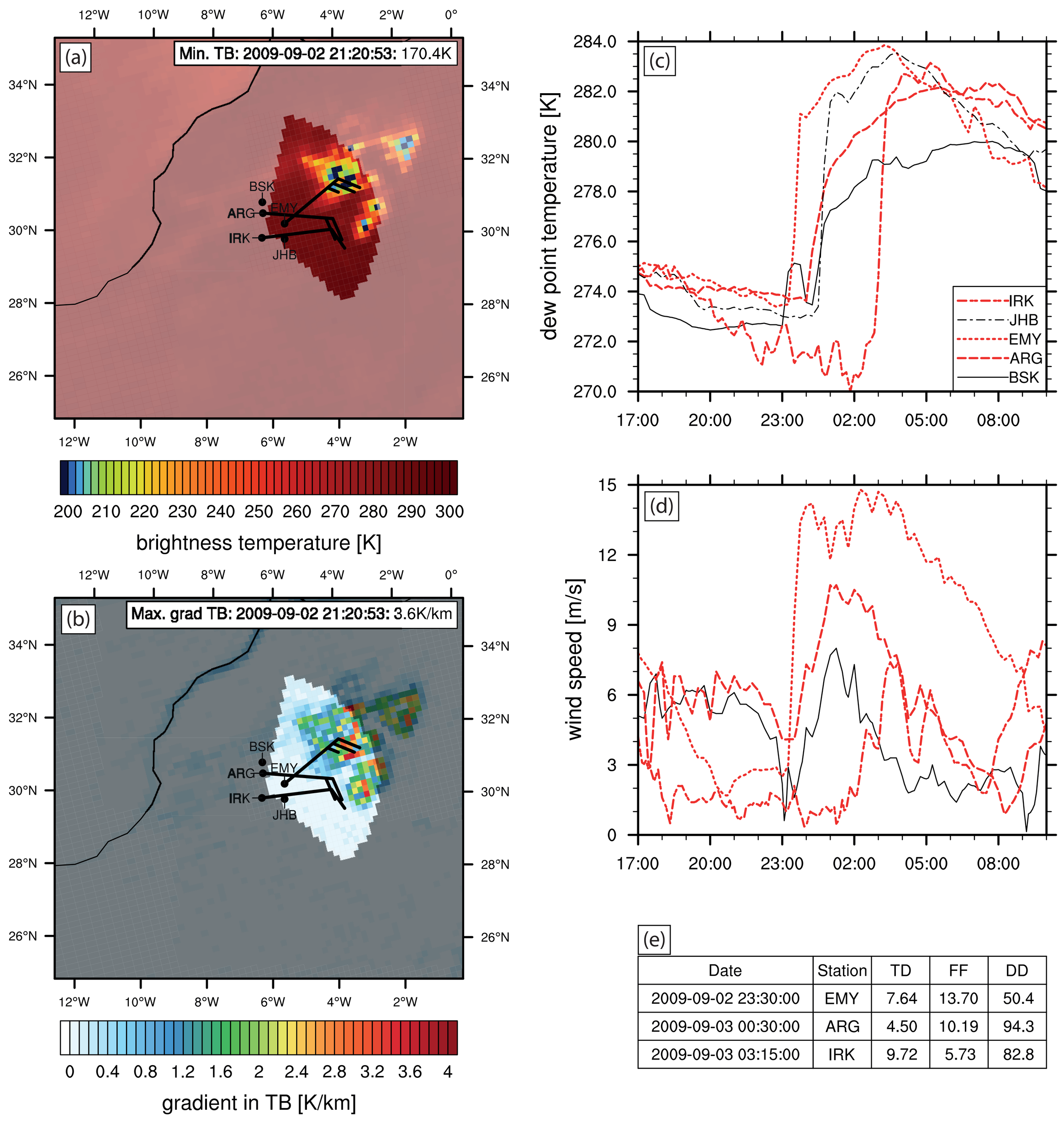

Date	Station	TD	FF	DD
2009-09-02 23:30:00	EMY	7.64	13.70	50.4
2009-09-03 00:30:00	ARG	4.50	10.19	94.3
2009-09-03 03:15:00	IRK	9.72	5.73	82.8

Figure 3: An example case detected by the automated algorithm in ground observations from the IMPETUS station network and satellite observations from MetOp-B in September 2009: (a) brightness temperatures measured in the 157 GHz channel; (b) horizontal gradient in brightness temperatures of the 157 GHz channel; (c) dew point temperature measured by AWSs; (d) wind speed measured by AWSs; red color in c and d indicate fulfilled criteria; (e) overview of measured values in tabular form (only stations that fulfill the criteria). The wedge-shaped brighter areas in (a) and (b) indicate the pixels used by the algorithm for convection screening. Source: Redl et al. (2015).

The detection method of convective cold pools combines automatic weather stations (AWSs) and SYNOP stations with microwave satellite measurements.

The algorithm consists of three steps:

- Preselection of cases based on station data.
- Grouping of contemporaneous cases from multiple stations into single events
- Confirming the existence of a nearby convective system based on microwave satellite data.

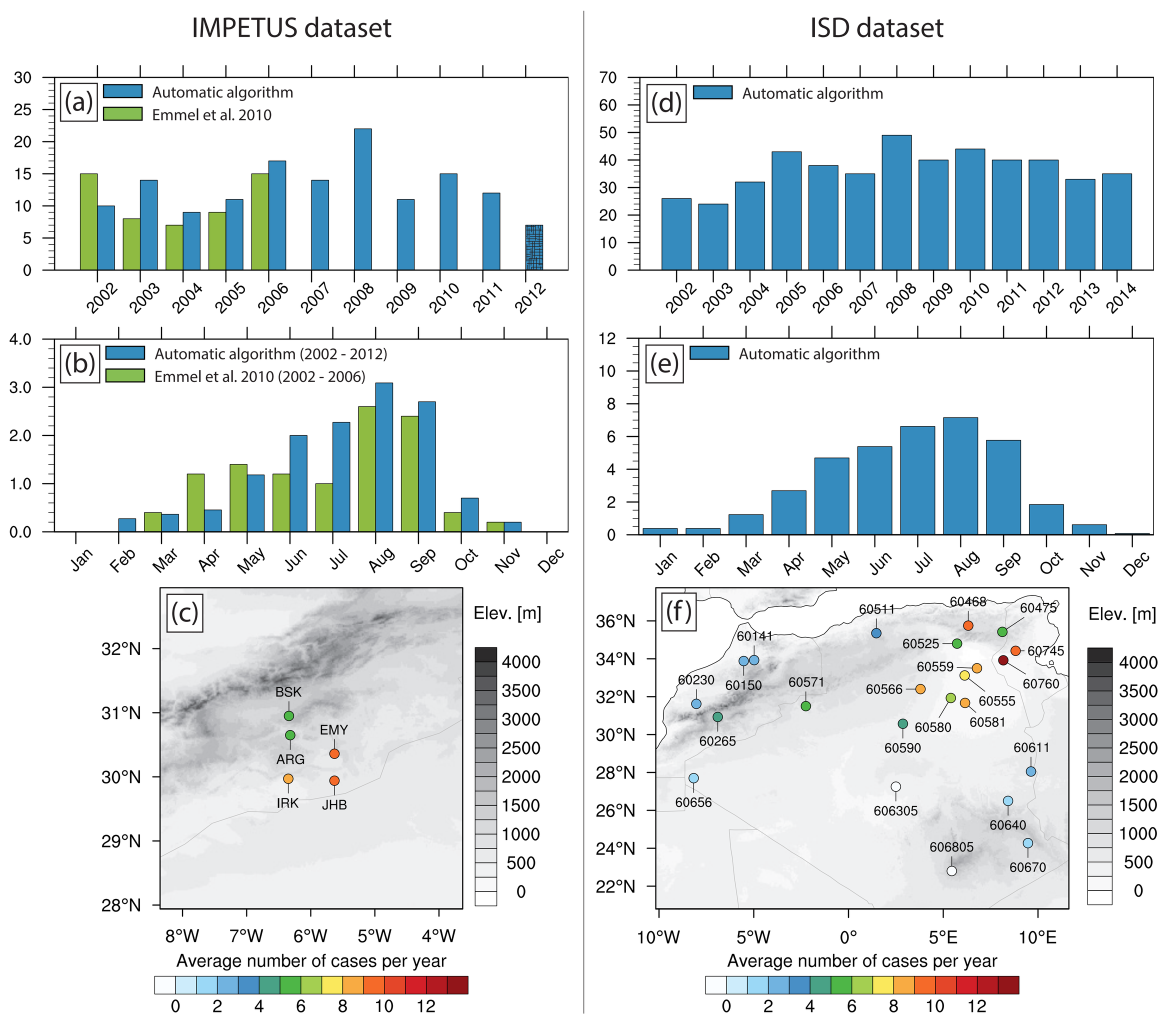

Figure 4: Climatology of cold pool events created from the IMPETUS dataset (a–c) and the ISD dataset (d–f): (a and d) Number of cases per year; (b and e) average number of cases per month; (c and f) average number of cases per station and year. For all panels only months with more than 80% data availability per station are included in the calculation. The hatching in (a) indicates incomplete data for 2012. Source: Redl et al. (2015).

Part 2: Impact of Individual Events on the SHL

Secondly, two convective periods in June 2011 and 2012 identified by the automated algorithm are simulated using the WRF model with a horizontal resolution of 3 km, which enables to explicitly resolve convection.

Method

- Create control runs with realistic convective cold pool for each case.
- Create manipulated model runs with removed cold pools. Manipulation are restricted to the area of the Atlas Mountains.
- Analyze differences between control runs and no-cold-pool runs.

Impact on Surface Pressure

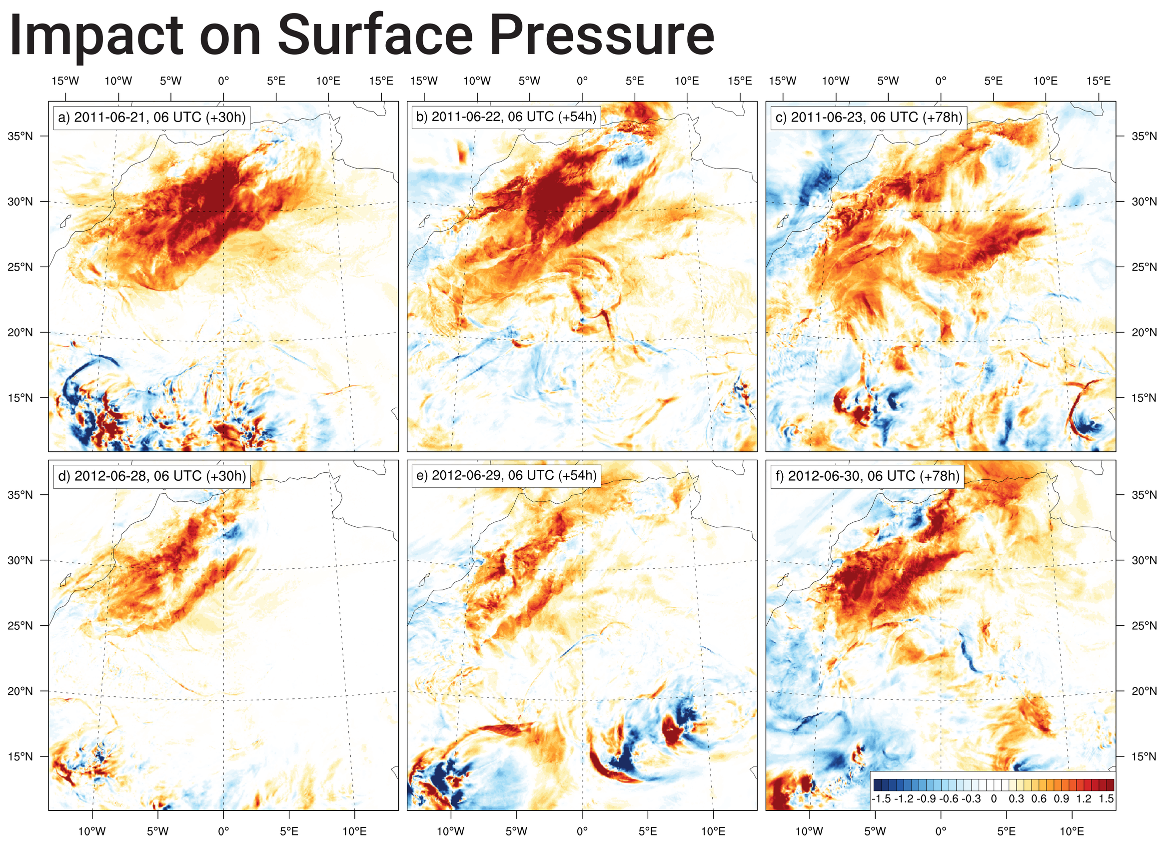

Figure 5: Difference in Mean sea level pressure (MSLP) between the control and the no cold-pool runs in hPa. Upper row: case 2011-06-20, lower row: case 2012-06-27. Source: Redl et al. (2016).

The most pronounced effect in P_{sfc} is visible in the morning hours. For case 1, the first morning shows the largest effect (Fig. 5a). An increase of at least 1 hPa is found over an area of approx. 580,000 km². The second case starts with a weaker increase in P_{sfc}, but the consecutive convective events produce an increase of at least 1 hPa over an area of approx. 392,000 km² on the third day (Fig. 5f).

Cold Pools as Moisture Source for the Desert

The accumulated contribution of the cold pools during both case studies is calculated using a tracer variable for moisture from evaporation of rain (Q_{ev}). During the whole 96h time period evaporation of rain is added and consumption by condensation is removed from Q_{ev}. The results for the end of both cases are shown vertically integrated in Fig. 6. Values of 5–9 kg m^{-2} are found where total column water vapor ranges from 16 to 41 kg m^{-2}.

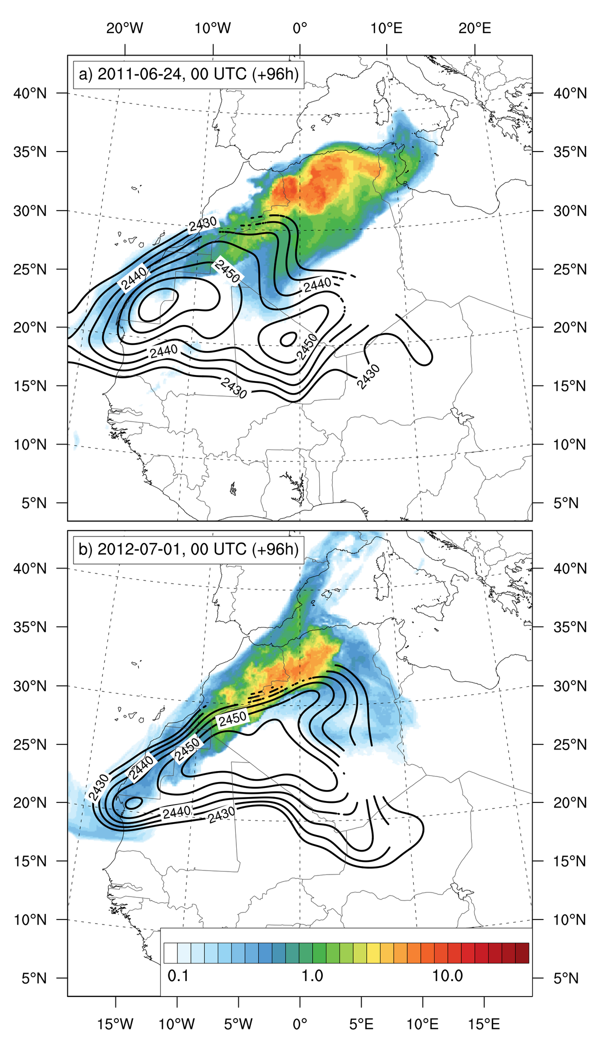

Figure 6: Vertically integrated water vapor created by evaporation of rain at the end of the control runs in kg m^{-2}. (a) case 1, (b) case 2. Source: Redl et al. (2016).

Modification of Surface Radiation Balance

Although a significant amount of moisture is transported into the desert, the net effect on the radiation balance in the first night is negative (Fig. 7a). This is explainable by the breakup of a very sharp surface inversion. Warm air is mixed down and the upwelling long-wave radiation is increased. This dynamic effect dominates in the first night, but the positive effect of the additional moisture (Fig. 7b) remains longer and modifies the radiation balance over days.

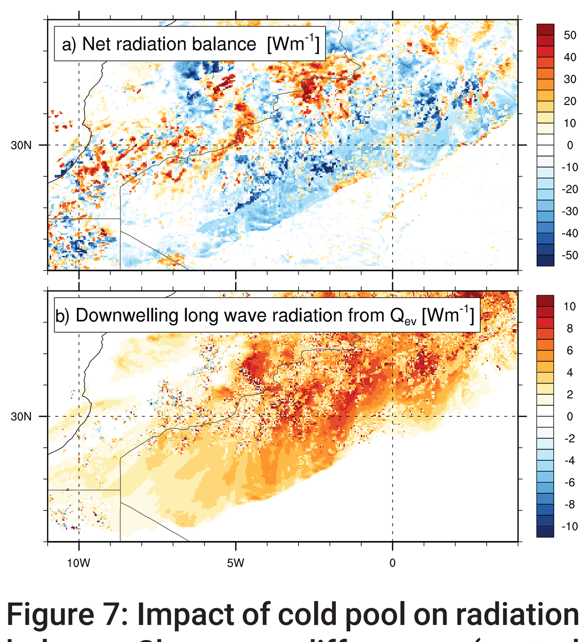

Figure 7: Impact of cold pool on radiation balance. Shown are differences (control run - no-cold pool) from case 1 at 00 UTC (+24 h). Source: Redl et al. (2016).